

$B \rightarrow \eta' + X$  and the QCD Anomaly  
David Atwood<sup>a</sup>, and Amarjit Soni<sup>b</sup>

- a) Theory Group, CEBAF, Newport News, VA 23606  
b) Theory Group, Brookhaven National Laboratory, Upton, NY 11973

**Abstract:** Mechanisms for the observed large  $Br(B \rightarrow \eta' + X_s)$  are examined. We propose that the dominant fraction of the  $B \rightarrow \eta' + X_s$  rate is due mainly to  $b \rightarrow sg^*$ , where  $g^*$  is an off-shell gluon, followed by  $g^* \rightarrow g\eta'$  via the anomalous coupling of the  $\eta'$  to two gluons. The calculated rate for  $B \rightarrow \eta' + X_s$  is in rough accord with experiment using a fairly constant glue-gluon- $\eta'$  form factor. This behavior of the form factor may be indicative of glueball dominance of the channel. Searches via the modes  $\eta' h^+ h^-$  ( $h = \pi$  or  $K$ ) may be worthwhile. Charmonia contributions [i.e  $B \rightarrow \eta_c, \psi(\rightarrow \eta' + X) + X_s$ ] can only account for at most 20% of the central value of the signal. Implications for  $B \rightarrow \eta' + X_d$  and for the corresponding  $\eta$  modes are also given.

# 1 Introduction

Recently CLEO has reported[1] a very large branching ratio for the inclusive production of  $\eta'$  (subject to the indicated cut):

$$\text{Br}(B \rightarrow \eta' + X; 2.2 \leq E_{\eta'} \leq 2.7\text{GeV}) = (7.5 \pm 1.5 \pm 1.1) \times 10^{-4} \quad (1)$$

In this Letter we report on possible mechanisms for this large signal. Two interesting origins are: (1)  $b \rightarrow s + g^*$  (where  $g^*$  is an off-shell gluon) followed by  $g^* \rightarrow \eta' + g$  due to the anomalous  $\eta'$ - $g$ - $g$  vertex. (2)  $b \rightarrow$  charmonia (e.g.  $\psi, \eta_c$ ) +  $X_s$  followed by  $\psi(\eta_c) \rightarrow \eta' + X$ . We discuss these below in turn.

## 2 Role of the Anomaly

We suggest that the dominant contribution to the observed large  $B \rightarrow \eta' + X$  signal is due to two crucial aspects of the Standard Model (SM). First, the SM predicts a very large branching ratio for the charmless  $b \rightarrow s$  penguin transition[2, 3]:

$$\text{Br}(B \rightarrow X_s) \sim 10^{-2} \quad (2)$$

(where  $X_s$  is a charmless state containing a  $s$ -quark). On the quark level these may be regarded as due to  $b \rightarrow sg^*$  transitions, where  $g^*$  is an off-shell gluon, and it is the gluons from this reaction that could be the source for the large  $\eta'$  production. This conversion of gluons to  $\eta'$  states may be accomplished through another important aspect of the SM, namely the QCD anomaly:

$$\partial_\mu j_5^\mu = \frac{3\alpha_s}{4\pi} G_{\mu\nu} \tilde{G}^{\mu\nu} + 2i \sum_{q=uds} m_q \bar{q} \gamma^5 q \quad (3)$$

where  $j_5^\mu$  is the singlet axial current[4]. Indeed it is the anomalous contribution to the divergence of the axial current that distinguishes the SU(3) singlet  $\eta_1$  state from the octet pseudo-goldstone  $\eta_8$  state. Intuitively it is the gluonic cloud of the  $\eta'$  which makes it appreciably heavier than the members of the octet:  $\pi$ ,  $K$  and  $\eta_8$ [5]. The physical  $\eta$  and  $\eta'$  states are related to these according to the mixing

$$\begin{aligned} \eta &= \cos \theta_\eta \eta_8 - \sin \theta_\eta \eta_1 \\ \eta' &= \sin \theta_\eta \eta_8 + \cos \theta_\eta \eta_1 \end{aligned} \quad (4)$$

where the mixing angle  $\theta_\eta$  is estimated[6] in the range of  $-10^\circ$  to  $-20^\circ$  so  $\eta'$  is dominantly  $\eta_1$ .

In order to model the gluonic coupling of the  $\eta_1$  we use an  $\eta'$ -glue-gluon effective vertex:

$$H(q_1^2, q_2^2, q_{\eta'}^2) \delta^{ab} \epsilon_{\mu\nu\alpha\beta} q_1^\mu q_2^\nu \epsilon_1^\alpha \epsilon_2^\beta \quad (5)$$

where  $q_1, q_2$  and  $\epsilon_1, \epsilon_2$  are the 4-momenta and polarizations of the two gluons and  $a, b$  are color indices. Thus the picture that we have for the inclusive  $\eta'$  production is a combination of  $b \rightarrow sg^*$  followed by  $g^* \rightarrow \eta'g$  as shown in Fig. 1. Indeed there have been many phenomenological attempts to quantify the gluonic content of the  $\eta'$ [7, 8]. In the effective vertex (5)  $H$  is a form factor that is a general function of the momenta,  $q_1^2, q_2^2$  and  $q_{\eta'}^2$ . If we expand this function in  $q_1^2$  and  $q_2^2$  at  $q_{\eta'}^2 = m_{\eta'}^2$ , the leading term is generated by the QCD anomaly. We will determine  $H(q_1^2 \approx 0, q_2^2 \approx 0, m_{\eta'}^2)$  by studying  $\psi \rightarrow \eta'\gamma$ .

As is well known, the  $b \rightarrow sg^*$  transition can be parameterized in the standard model (in the limit  $m_s \rightarrow 0$ ) by the induced chromo-electric and chromo-magnetic form factors [2, 3]:

$$\begin{aligned} \Lambda_{e,\mu}^{b \rightarrow s} &= +\frac{G_F}{\sqrt{2}} \sum_{i=uct} v_i \bar{s}(\lambda^a/2) [F_1^i(q^2)(\gamma_\mu q^2 - q_\mu \not{q})L] b \\ \Lambda_{m,\mu}^{b \rightarrow s} &= -\frac{G_F}{\sqrt{2}} \frac{g_s m_b}{2\pi^2} \sum_{i=uct} v_i \bar{s}(\lambda^a/2) [F_2^i(q^2) i\sigma_{\mu\nu} q_\nu R] b \end{aligned} \quad (6)$$

where  $v_i = V_{is}^* V_{ib}$ ,  $g_s$  is the QCD coupling constant,  $q = p_b - p_s$  is the outflowing gluon momentum,  $\lambda^a$  are the Gell-Mann matrices,  $R = (1 + \gamma^5)/2$  and  $L = (1 - \gamma^5)/2$ .

Using Eq. 6 and Eq. 5 we can deduce the differential decay rate for  $b(p_b) \rightarrow \eta'(q_{\eta'})s(p_s)g(k)$ :

$$\frac{d^2\Gamma}{dsdt} = \frac{H^2 v_t^2 G_F^2}{384\pi^3 m_b^3} [\hat{F}^2(2V - (m_b^2 - s)W/2) + 2\hat{G}^2(m_b^2 - s)V + 4m_b \hat{F} \hat{G} V] \quad (7)$$

Here  $s = (q_{\eta'} + k)^2 \equiv q^2$ ,  $t = (p_s + k)^2$  and  $u = (p_s + q_{\eta'})^2$ ,  $V = (stu - m_{\eta'}^2 m_b^2 t)/4$ ,  $W = -(s - m_{\eta'}^2)^2/2$ ,  $\hat{G} = g_s m_b f_2/(2\pi^2 s)$  and  $\hat{F} = f_1 - m_b \hat{G}$ . We have neglected the small contribution of the  $u$ -quark and defined  $f_i = F_i^t - F_i^c$ .

We can now readily calculate the rate for  $b \rightarrow sg\eta'$  if we assume that

$f_i, H$  are roughly constant as a function of  $s = q^2$ :

$$\Gamma(b \rightarrow s\eta'g) = \frac{m_b^2 H^2 \Gamma_0}{8} (f_i^2 \tau_0(x) + \frac{g_s}{2\pi^2} f_i f_2 \tau_1(x) + \frac{g_s^2}{4\pi^4} f_2^2 \tau_2(x)) \quad (8)$$

where  $\Gamma_0 = |V_{cb}|^2 G_F^2 m_b^5 / (192\pi^3)$ ,  $x = m_{\eta'}^2 / m_b^2$  and  $\tau_i(x)$  is given by:

$$\begin{aligned} \tau_0(x) &= x^2 \log(1/x) + \frac{1}{60} (1-x)(3 - 27x - 47x^2 + 13x^3 - 2x^4) \\ \tau_1(x) &= 2x^2(2x+3) \log(1/x) + \frac{1}{6} (1-x)(1 - 11x - 47x^2 - 3x^3) \\ \tau_2(x) &= -x(3x+2) \log(1/x) + \frac{1}{12} (1-x)(3 + 47x + 11x^2 - x^3) \end{aligned} \quad (9)$$

The value of  $\Gamma_0/\Gamma_B$  where  $\Gamma_B$  is the total width of the  $B$ , may be ascertained, at leading order, by factoring the phase space effects of the  $c$ -quark into the semi-leptonic branching ratio so that if  $x_c = (m_c/m_b)^2$  then for  $l = e, \mu$ :

$$\Gamma(\overline{B} \rightarrow l\overline{\nu}_l X_c) = ((1 - 8x_c + x_c^2)(1 - x_c^2) + 12x_c^2 \log \frac{1}{x_c}) \Gamma_0 \quad (10)$$

Thus using  $\Gamma(\overline{B} \rightarrow l\overline{\nu}_l X_c)/\Gamma_B = 0.1$ [6] we obtain  $\Gamma_0/\Gamma_B \approx 0.2$ .

Next to deduce  $H$  we describe  $\psi \rightarrow \gamma\eta'$  by assuming that the  $\psi$  is a weakly bound state of  $c\bar{c}$  quarks[9] in conjunction with the coupling in Eq. 5 [see Fig. 2]. Explicit calculations then show that the amplitude is dominated by on-shell gluons leading to

$$m_{\eta'}^2 H^2 \cos^2 \theta_\eta = \frac{\pi\alpha}{2\alpha_s^2} \frac{\Gamma(\psi \rightarrow \gamma\eta')}{\Gamma(\psi \rightarrow e^+e^-)} \frac{(1-r)(1+r)^2}{r^3 \log^2 r} \quad (11)$$

where  $r = (m_{\eta'}/m_\psi)^2$ .

We thus arrive at  $H(0, 0, m_{\eta'}^2) \sim 1.8 GeV^{-1}$  for  $\alpha_s(m_\psi) = .25$  and  $\theta_\eta = -17^\circ$ [10, 6] and other data from [6]. As mentioned before, there is considerable uncertainty in the value of  $\theta_\eta$ . However, due to our normalization with respect to  $\psi \rightarrow \gamma\eta'$ , the rate for  $b \rightarrow s\eta'g$  is independent of the precise value of  $\theta_\eta$ . This value of  $H$  is in rough accord with the coupling which one expects from an anomalous QCD contribution to the  $g$ - $g$ - $\eta'$  vertex[4, 11].

Finally, in order to estimate the rate for  $b \rightarrow \eta'gs$  we need to know the value of  $F_1$  and  $F_2$ .  $F_1$  is calculated at leading order, for instance, in [2]

where  $F_1 \approx -.20$ . We can infer that QCD corrections do not effect this result greatly by considering next-to-leading order (NLO) calculations of penguin operators in [3, 12]. To do this we expand in terms of their  $O_i$  operators:

$$\begin{aligned}
c_4 O_4 + c_6 O_6 &= (1/2)(c_6 - c_4)(O_6 - O_4) + (1/6)(c_6 + c_4)(O_3 + O_5) \\
&+ (c_6 + c_4) \left[ (\bar{b}_a \gamma^\mu L \frac{\lambda_{ab}^i}{2} s_b) \sum_q (\bar{q}_c \gamma_\mu \frac{\lambda_{cd}^i}{2} q_d) \right] \quad (12)
\end{aligned}$$

where  $c_i$  are the appropriate Wilson Coefficients of  $O_i$  [12, 13]. We note that the last term corresponds to a color octet exchange with the same quantum numbers as a gluon. Thus we attribute it to the exchange of a single effective gluon from a penguin inferring that  $F_1 = 4(c_4 + c_6)/g_s$  which gives a result that agrees with the above to  $O(20\%)$ . For instance, using the leading order calculation in [13] with  $\Lambda_{\overline{ms}}^{(5)} = 225 MeV$  so  $\alpha_s = .21$  we obtain  $F_1 = -.168$ . The quantity  $F_2$  may be taken directly from this calculation since  $F_2 = c_{8G} = .143$ .

We can now readily estimate the branching ratio for  $b \rightarrow s\eta'g$ . Using  $F_1 = -.168$ ,  $H \cos \theta_\eta = 1.7 GeV^{-1}$  and  $\Gamma_0/\Gamma_B = .2$  and taking  $m_b = 4.8 GeV$  we get  $1.9 \times 10^{-3}$  if just the electric form factor is used while the presence of the magnetic form factor increases this result by about 50% yielding  $Br(b \rightarrow s\eta'g) \sim 2.8 \times 10^{-3}$ .

The results quoted in [1] however contain an acceptance cut designed to reduce the background from events with charmed mesons[14]. This cut requires that the energy of the  $\eta'$ ,  $E_{\eta'} \geq 2.2 GeV$  which is equivalent to the cut in the recoil mass  $m_{rec} \leq 2.35 GeV$

In order to understand the  $m_{rec}$  spectrum from a  $B$ -meson, one must factor in the fermi motion of the  $b$ -quark with respect to the meson. For this purpose, following previous works [15], we assume that the momentum of the  $b$ -quark has a probability distribution of the form

$$P \propto e^{-|p|^2/\beta^2}. \quad (13)$$

which is suggested by a harmonic-oscillator like wave function. Fits to the semileptonic decay spectrum at CLEO[16] suggest a value of  $\beta = 0.287 GeV$ ;  $m_b = 4.87 GeV$ . In our results we consider  $\beta = .15 - .45 GeV$ , though in most cases the branching ratios are not strongly dependent on  $\beta$ . When the cut is imposed however, the fraction passing the cut is strongly dependent

on  $m_b$ . Following CLEO ( $b \rightarrow s\gamma$ ) [16] we vary  $m_b$  over the range of 4.7 to 4.9 GeV. Using  $\beta = 0.3$  GeV we find that for  $m_b = 4.7$  GeV the branching fraction which passes the cut is  $6.7 \times 10^{-4}$  while if  $m_b = 4.9$  GeV then the corresponding branching fraction is  $9.8 \times 10^{-4}$ . Furthermore the proportion of events passing the cut varies from  $\zeta_{cut}(E_{\eta'}) \approx 25 - 33\%$ .

Thus, taking  $m_b = 4.8$  GeV and identifying  $b \rightarrow sg\eta'$  as the dominant contribution[11] to the inclusive process we find that after including the experimental cuts:

$$Br(B \rightarrow \eta' X) \approx 8.2 \times 10^{-4} \quad (\text{including cuts}) \quad (14)$$

which is in rough accord with the experimental result given in Eq. 1. If we include a 150 MeV uncertainty in  $m_b$  and 0.04 in  $\alpha_s$  then in this model the above number varies by about 30%. Fig. 3 shows the  $m_{rec}$  distribution for  $\beta = 0.15, 0.3$  and  $0.45$  GeV,  $m_b = 4.8$  GeV as well as the case  $\beta = 0.3$  GeV for  $m_b = 4.6$  GeV. As can be seen, for a fixed  $m_b$ , there is some variation in these spectra with  $\beta$  only in the region  $m_{rec} \leq 1.5$  GeV[1]. The reason for the large dependence on  $m_b$  is readily apparent since as  $m_b$  decreases the curve shifts to the right and the proportion of events falling below the  $m_{rec}$  cut corresponding to  $E_{\eta'} = 2.2$  GeV rapidly drops.

Although there are several uncertain parameters in the calculation ( $\alpha_s, m_b, \beta \dots$ ) it is quite remarkable that an approximate constant form factor  $H$  leads to a rate (Eq. (14)) that roughly agrees with experiment (Eq. (1)) as one of the gluons is considerably off-shell,  $\langle q_1^2 \rangle \sim 10$  GeV<sup>2</sup>. This behavior of the form factor may be an indication that it is dominated by the presence of gluonic states in the two gluon channel. The large  $\eta'$  signal offers a unique possibility, in any case, to search for such states through the modes, for example,

$$\text{Glueball} \rightarrow \eta' + h^+ + h^- \quad (15)$$

where  $h = \pi$  or  $K$ . Thus it may be worthwhile to closely study the invariant mass distribution of  $(q_{\eta'} + q_{h^+} + q_{h^-})^2$  in the data sample.

### 3 Contribution from Charmonia

Charmonia contributions (See Fig. 4) can be subdivided into three categories:

1. The most important of this class of contributions is from  $b \rightarrow \eta_c + s$  followed by  $\eta_c \rightarrow \eta' + X$ . (See Fig. 4a). The experimental acceptance cut plays a very important role here. It essentially eliminates all contributions from a multi-body state  $X$  and only a single particle or resonance ( $X$ ) remains viable. Important examples of  $X$  are:  $\sigma, \eta, \omega, \eta' \dots$  [17]. We find  $\zeta_{cut}(m_X \sim 2m_\pi) \sim 20\%$ ,  $\zeta_{cut}(m_X \sim m_\eta) \sim 15\%$ ,  $\zeta_{cut}(m_X \sim m_\omega) \sim 10\%$  and  $\zeta_{cut}(m_X \sim m_\phi) \sim 1.5\%$ . From the measured branching ratios of  $\eta_c$  into such states we estimate that their sum,  $\sum_i Br(\eta_c \rightarrow \eta' X_i) \sim 10\%$ . Using  $Br(B \rightarrow \eta_c + X_s) \sim 7.0 \times 10^{-3}$  [6, 18], we thus see that, from this mechanism:

$$\begin{aligned}
Br(B \rightarrow \eta' + X_s) &= Br(B \rightarrow \eta_c + X_s) \times \sum_i Br(\eta_c \rightarrow \eta' + X_i) \times \zeta_{cut} \\
&\sim 1.1 \times 10^{-4}.
\end{aligned} \tag{16}$$

2. Next we consider  $b \rightarrow \eta_c^*(\rightarrow \eta') + s$ . (See Fig. 4b). We view this contribution to arise through a mixing of  $\eta_c$  and  $\eta'$ . Such a mixing is predominantly driven by the two gluon intermediate state. It is very difficult to see why this mixing angle should be bigger than a degree[11]. Thus  $Br(b \rightarrow \eta_c^*(\rightarrow \eta') + s) = \sin^2 \theta_{\eta_c} \times Br(b \rightarrow \eta_c + s) \leq 3 \times 10^{-6}$  and is negligible.
3. Finally there is also the possibility that  $b \rightarrow \psi + s$  followed by  $\psi \rightarrow \eta' + X$ . [See Fig. 4a] Again, the acceptance cut effectively requires that  $X$  be a single particle state. Thus possible examples of  $X$  are  $\gamma, \omega, \phi$  etc. The corresponding branching ratios are expected to be very small, each is  $\leq 0.5\%$  [6], suggesting that  $\sum_i Br(\psi \rightarrow \eta' + X_i) \sim 2\%$ . We thus estimate from  $b \rightarrow \psi + s$  the resulting contribution is  $Br(B \rightarrow \eta' + X_s) \sim 3 \times 10^{-5}$ .

Thus the main charmonia contribution is via  $B \rightarrow \eta_c + X_s, \eta_c \rightarrow \eta' + X$  with an effective  $Br(B \rightarrow \eta' + X_s) \sim 1.1 \times 10^{-4}$  (including cuts), which is at most 20% of the observed central value.

Experimentally, the charmonia contributions coming via cascade decays of  $\psi$  and or  $\eta_c$  can, in principal, be separated by studying the invariant mass distributions of the expected final states, such as  $\eta' + \eta(\eta', \phi, \omega, \gamma, \pi\pi, KK \text{ etc})$ , which should cluster around  $m_{\eta_c}$  and/or  $m_\psi$ .

Note also that while the  $\eta_c - \eta'$  mixing is expected to make a negligible contribution it tends to have a distinctive  $m_{rec}$  distribution which is quasi-two-body; it peaks around  $m_{rec} \sim 1.5 GeV$  and diminishes rapidly either side of this region.

## 4 Other Mechanisms

In passing we note that there are other mechanisms[11] for making  $\eta'$  in  $B$  decays:

1. There is a  $b \rightarrow s\bar{s}s$  penguin process where the  $\bar{s}$ -quark from the gluon may pair with one of the  $s$ -quarks as shown in Fig. 5a.
2. There is a  $b \rightarrow s\bar{u}u$  (or  $s\bar{d}d$ ) penguin process where the light quarks pair as shown in Fig. 5b.
3. There is a  $b \rightarrow su\bar{u}$  (and also  $b \rightarrow sd\bar{d}$ ) penguin process where the  $u(d)$  can pair with the spectator  $\bar{u}(\bar{d})$  to make the  $\eta'$  as shown in Fig. 5c.
4. There is a  $b \rightarrow sgg$  penguin sub-process followed by  $gg \rightarrow \eta'$  shown in Fig. 5d.
5. The  $\eta'$  may also be produced through a  $b \rightarrow su\bar{u}$  tree graph shown in Fig. 5e.

Using the NLO effective Hamiltonian [12] and vacuum saturation we can estimate the contributions of Fig. 5a and Fig. 5b. This is straightforward for all of the operators except for the contributions of  $O_5$  and  $O_6$ . In these cases we need to know

$$G_{\eta_1}(q_i) = \sqrt{3} \langle 0 | \bar{q}_i \gamma^5 q_i | \eta_1 \rangle \quad (17)$$

Due to the presence of the anomalous contribution there is no direct way to deduce the value of  $G_{\eta_1}$  but a reasonable estimate is perhaps that  $G_{\eta_1} = G_\pi$  where

$$G_\pi = \langle 0 | \bar{u} \gamma^5 d | \pi^+ \rangle \approx m_\pi^2 f_\pi / (m_u + m_d). \quad (18)$$

Using  $m_u + m_d \approx 15 MeV$ , Fig. 5a together with Fig. 5b give  $\sim 7.5 \times 10^{-6}$ .

We estimate the three-body penguin (Fig. 5c) to contribute about  $2 \times 10^{-5}$  which gives  $1 \times 10^{-5}$  with the cut implemented. In this estimate, we have



used as normalization, the CLEO central value for  $Br(B^0 \rightarrow \pi^- \ell^+ \nu_\ell) = (1.8 \pm .4 \pm .3 \pm .2) \times 10^{-4}$  [1].

Simma and Wyler [19] consider gluball production from  $b \rightarrow sgg$ . Their calculation can be adapted to the  $\eta'$  (Fig. 5d) yielding about  $1 \times 10^{-5}$ .

The  $b \rightarrow su\bar{u}$  tree graph contribution (Fig. 5e) may be estimated to be about  $5 \times 10^{-6}$  which becomes about  $2.6 \times 10^{-6}$  with cuts. This contribution is only to  $B^+$ ; the  $B^0$  decay via the tree is color suppressed. Thus when one averages over  $B^0$  and  $B^\pm$  this is effectively reduced by a factor of about 2.

Thus, for  $b \rightarrow \eta' + X_s$  all of these processes are found to be appreciably less than the production through the anomaly coupling (Fig. 1) and indeed not even competitive with the charmonia contribution, Eq. (16). We estimate that these subdominant processes will not alter the main contribution by more than about 10%; therefore, for now we can safely ignore them [11].

Inclusive  $\eta$  production,  $B \rightarrow \eta + X_s$ , will in general proceed through the processes which we have discussed above for the  $\eta'$ . The production through the gluon mechanism of Fig. 1 is suppressed by approximately  $\tan^2(\theta_\eta)$  (up to small additional corrections due to the difference in mass). Thus if  $\theta_\eta = -17^\circ$  then the total branching ratio with this mechanism is  $2.6 \times 10^{-4}$  while with a cut of  $E_\eta > 2.2\text{GeV}$  the branching fraction is  $8 \times 10^{-5}$ .

Next we consider the charmonia contribution to  $\eta$ . From Ref. [6] we see that in  $\eta_c, \psi$  decays, the branching ratios of final states with  $\eta$  are roughly the same as those with  $\eta'$ [20]. This leads us to suggest that, from charmonia,  $Br(B \rightarrow \eta + X_s) \sim 7.3 \times 10^{-5}$ .

The mechanisms Fig. 5a and 5b for the  $\eta$  give  $1.3 \times 10^{-5}$ . The kinematics are such that virtually all of the events will pass the cut. The process shown in Fig. 5c gives a total branching fraction of about  $3.6 \times 10^{-5}$  of which about  $1.3 \times 10^{-5}$  passes the cut. The tree process gives  $\approx 3 \times 10^{-6}$  (with cuts) but only from  $B^\pm$  decays thus effectively reducing this by a factor of 2 when  $B^\pm$  and  $B^0$  are averaged.

It is also interesting to consider the situation when one replaces the  $b \rightarrow s$  penguin with a  $b \rightarrow d$  penguin and thus contemplates the inclusive process  $b \rightarrow \eta' X_d$ .

With the exception of the tree graph (Fig. 5e) and the charmonium, all of the processes considered above will scale with  $r_{ds}^2 = |V_{td}/V_{ts}|^2 \sim O(\lambda^2)$  where  $\lambda = \sin \theta_c \simeq .22$  while the charmonium processes will scale like  $\lambda^2$ .

The tree graph, on the other hand, leads to  $\Gamma(b \rightarrow d\bar{u}u)/\Gamma(b \rightarrow s\bar{u}u) \approx 1/\lambda^2$  so the contribution of this process to the branching ratio of  $b \rightarrow \eta' X_d$

is about  $5.4 \times 10^{-5}$  (including cuts). Therefore this may be expected to provide the dominant contribution to  $B^+ \rightarrow \eta' + X_d$ . For  $B^0$  this process is color suppressed. So from the tree, averaging over the two,  $B \rightarrow \eta' + X_d \sim 2.7 \times 10^{-5}$  (with cuts).

## 5 Summary and Outlook

Table 1 summarizes the expected rates, for individual mechanisms, as well as the total for the four final states of interest:  $\eta'X_s$ ,  $\eta'X_d$ ,  $\eta X_s$  and  $\eta X_d$ . For the  $\eta'X_s$ , the branching ratio is about  $3.5 \times 10^{-3}$  and is about  $2.5 \times 10^{-4}$ ,  $1 \times 10^{-3}$  and  $1.4 \times 10^{-4}$  respectively for the other three, assuming for simplicity,  $|V_{td}/V_{ts}|^2 = 0.05$ . The current CLEO acceptance cuts [Eq. (1)] affect the anomalous contribution (Fig. 1) more severely (about a factor of 3 to 3.5) than the tree contribution (about a factor of two). As indicated in the Table the anomalous graph is the dominant mechanism contributing perhaps about 86% of the total for  $\eta'X_s$ . It contributes about 55%, 44% and 10% to  $\eta'X_d$ ,  $\eta X_s$  and  $\eta X_d$  respectively.

An especially notable feature of the numbers in the Table is that the rates with cuts for the other modes ( $\eta X_d$ ,  $\eta'X_d$  and  $\eta X_s$ ) are also predicted to be quite large, i.e.  $(0.4 \text{ to } 1.8) \times 10^{-4}$ , although none is as high as the  $\eta'X_s$ . Their searches are eagerly awaited as comparison with experiment will be very instructive.

In closing, it is important to note that the  $b \rightarrow s\eta'g$  mechanism should be regarded as the dominant contributor to the multiparticle inclusive process  $B \rightarrow \eta' + X_s$ , where  $X_s$  is a kaon together with at least one pion. It is expected [11] to make a negligible contribution to the exclusive two body mode ( $B \rightarrow \eta' + K$ ). We recall that experimentally  $B \rightarrow \eta' + K$  is seen [1] to be about 10% of the inclusive signal  $B \rightarrow \eta' + X_s$ . To facilitate contact with theoretical models, it may be better if the two body signal is not included in the inclusive rate, Eq. 1.

It is extremely interesting that the  $\eta'$  becomes such an effective probe of the  $b \rightarrow sg^*$  process. It has long been known that these charmless final states have a very large branching ratio [2]. The  $\eta'$  could therefore become a very powerful tool for gluonia searches and for illuminating our understanding of the penguin dynamics, and, in particular for the quest for direct CP violation as the same final states are expected to be rich in CP asymmetries[21].

**Acknowledgements:** The authors would like to acknowledge useful discussion with Jim Alexander, Bruce Behrens, Tom Browder, José Goity, Nathan Isgur, Alex Kagan, Peter Kim, Bill Marciano, Ron Poling, Laura Reina, Jon Rosner and Sheldon Stone. This research was supported in part by the U.S. DOE contracts DC-AC05-84ER40150 (CEBAF), DE-AC-76CH00016 (BNL).

## References

- [1] P. Kim, [CLEO] Talk at FCNC 1997, Santa Monica, CA (Feb 1997); See also the [CLEO] talks by B. Behrens and by R. Poling at *B* Physics and CP Violation, Waikiki, HI (March 1997).
- [2] W. S. Hou, A. Soni and H. Steger, Phys. Rev. Lett. **59**, 1521 (1987); W. S. Hou, Nucl. Phys. **B308**, 561 (1988).
- [3] R. Grigjanis, P. O'Donnell, M. Sutherland and H. Navelet, Phys. Lett. **B224**, 209 (1989); B. Grinstein, R. Springer and M. Wise, Phys. Lett. **B202**, 138 (1988); A. Buras, M. Jamin, E. Lautenbacher and P. Weisz, Nucl. Phys. **B370**, 69 (1992); M. Ciuchini, E. Franco, G. Martinelli, L. Reina and L. Silvestrini Phys. Lett. **B344**, 137 (1994).
- [4] See e.g. D. V. Schroeder and M. Peskin *An Introduction to Quantum Field Theory*, Addison-Wesley (1995); C. Itzykson and J. B. Zuber, *Quantum Field Theory*, McGraw-Hill (1980).
- [5] A. DeRujula, H. Georgi and S. Glashow, Phys. Rev. **D12**, 147 (1975); N. Isgur, Phys. Rev. **D13** (1976); E. Witten, Nucl. Phys. **B156**, 269 (1979).
- [6] Particle Data Group, Phys. Rev. **D54**, 1 (1996).
- [7] J. Rosner, Phys. Rev. **D27**, 1101 (1983).
- [8] P. Ball, J.-M. Frère and M. Tytgat, Phys. Lett. **B365**, 367 (1996) and references therein.
- [9] T. Appelquist and H. D. Politzer, Phys. Rev. **D12**, 1404 (1975).
- [10] N. Isgur in Ref. [5].

- [11] For further details see D. Atwood and A. Soni, in preparation.
- [12] G. Kramer, R. Palmer and H. Simma, Z. Phys. C**66**, 429 (1995).
- [13] G. Buchalla, A. J. Buras and M. E. Lautenbacher, Rev. Mod. Phys. **68**, 1125 (1996).
- [14] A large background is expected from decays of the type  $B \rightarrow D_s + D + X$  followed by  $D_s \rightarrow \eta' + Y$  (e.g.  $D_s \rightarrow \eta' + \rho$ ). The experimental acceptance cut in Eq. (1) eliminates most of these.
- [15] See A. Ali and C. Greub, Phys. Lett. B**259**, 182 (1991) and references therein; N. Isgur, D. Scora, B. Grinstein and M. Wise, Phys. Rev. D**39**, 799 (1989); G. Altarelli *et. al.*, Nucl. Phys. B**208**, 365 (1982).
- [16] M. S. Alam *et. al.* (CLEO Collab.), Phys. Rev. Lett. **74**, 2885 (1995).
- [17] We are using the notation  $\sigma$  to mean a  $0^{++}$ , broad resonance in the  $2\pi$  channel, with mass  $\sim 400$ – $1200$  MeV and width  $600$ – $1000$  MeV [See Ref. 6].
- [18] N. G. Deshpande and J. Trampetic, Phys. Lett. B**339**, 270(1994).
- [19] H. Simma and D. Wyler, Nucl. Phys. B**344**, 253 (1990).
- [20] In the case of the charmonia mechanism giving rise to  $\eta$ , the cuts tend to reduce the signal more than in the case of  $\eta'$ . Thus  $\zeta_{cut}(m_X \sim 2m_\pi) \sim 14\%$ ,  $\zeta_{cut}(m_X \sim m_\eta) \sim 10\%$ ,  $\zeta_{cut}(m_X \sim m_\omega) \sim 5\%$  and  $\zeta_{cut}(m_X \sim m_\phi) \sim .25\%$ . We will therefore use an average cut of 10% for the  $\eta$  compared to 15% for the  $\eta'$ .
- [21] M. Bander, D. Silverman and A. Soni, Phys. Rev. Lett. **43**, 242 (1979); N.G. Deshpande and A. Soni, Proc. Snowmas '86, p. 58; J. M. Gerard and W. S. Hou, Phys. Rev. D**43**, 2909 (1991); H. Simma, G. Eilam and D. Wyler, Nucl. Phys. B**352**, 367 (1991); G. Kramer, R. Palmer and H. Simma (ref. [12]) L. L. Chau, H. Y. Cheng, W. K. Sze, B. Tseng and H. Yao, Phys. Rev. D**45**, 3143 (1992) and references therein.

## Figure Captions

Figure 1: The main mechanism for the inclusive  $\eta'$  production:  $b \rightarrow sg^*$  graph followed by  $g^* \rightarrow g\eta'$  where the black circle denotes the anomalous  $gg\eta'$  coupling.

Figure 2:  $\psi \rightarrow \gamma gg$  followed by  $gg \rightarrow \eta'$  via the anomalous  $gg \rightarrow \eta'$  vertex.

Figure 3: Recoil mass distribution for  $B \rightarrow X_s\eta'$  from the sub-process  $b \rightarrow g\eta's$ . The events falling to the left of the vertical line pass the  $E_{\eta'} > 2.2\text{GeV}$  cut. For  $m_b = 4.8\text{ GeV}$ , the solid curve shows the distribution for  $\beta = 0.3\text{GeV}$  while in the region  $m_{rec} < 1.6\text{GeV}$  the distributions for  $\beta = 0.15\text{GeV}$  (dashed) and  $\beta = 0.45\text{GeV}$  (dotted) are also shown. For  $m_b = 4.6\text{ GeV}$  and  $\beta = 0.3\text{ GeV}$  the  $m_{rec}$  distribution is shown by the dot-dashed curve. Each of the above curves is normalized so that its integral is unity.

Figure 4: Charmonia contributions: a)  $b \rightarrow \psi, \eta_c + s$  followed by  $\psi, \eta_c \rightarrow \eta' + X$ . b)  $b \rightarrow \eta_c^*(\rightarrow \eta') + s$ ;  $\mathbf{X}$  denotes  $\eta_c \leftrightarrow \eta'$  mixing.

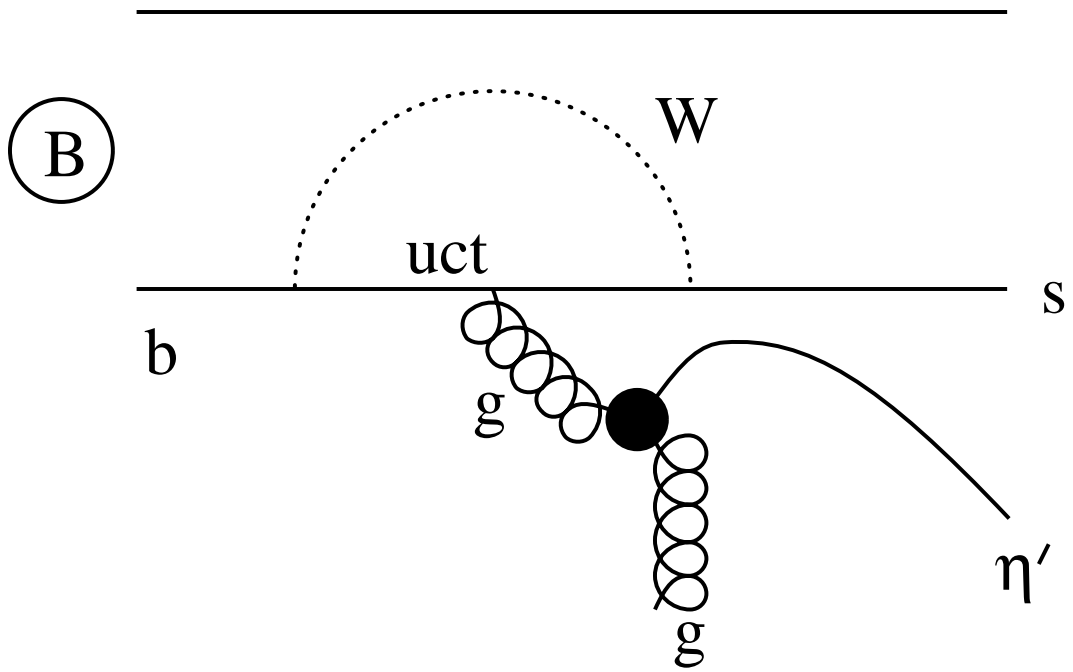
Figure 5: Feynman diagrams for the sub-dominant contributions to  $B \rightarrow \eta' + X_s$ . The four quark penguin operators (i.e.  $O_3 - O_6$ ) are represented by hexagons. The diagrams shown are: (a) the  $b \rightarrow s\bar{s}s$  process where the  $\bar{s}$ -quarks may combine with either of the  $s$ -quarks to form an  $\eta'$ ; (b) the  $b \rightarrow s\bar{u}u$  or  $s\bar{d}d$  process where the  $u\bar{u}$  ( $d\bar{d}$ ) forms the  $\eta'$ ; (c) A typical penguin graph producing two gluons that fuse to form a  $\eta'$ ; (d) a  $b \rightarrow s\bar{u}u$  or  $s\bar{d}d$  process where the light quark combines with the spectator; (e) the  $b \rightarrow su\bar{u}$  tree process.

Table 1: Contributions from different mechanisms to the  $Br(B \rightarrow \eta'(\eta) + X_{s,d})$  in units of  $10^{-5}$ . The number from each graph is given along with the total, without cuts. The effect of CLEO acceptance cuts on the total is also indicated. Note  $r_0^2 = 20|V_{td}/V_{ts}|^2$ .

Mechanism	Type	$\eta' X_s$	$\eta' X_d$	$\eta X_s$	$\eta X_d$
Fig. 1	Anomaly	280	$14r_0^2$	26	$1.3r_0^2$
Fig. 4	Charmonia	70	3.4	70	3.4
Fig. (5a + 5b)	penguin-4q-op	0.75	$0.04r_0^2$	1.3	$0.07r_0^2$
Fig. 5c	penguin-4q-op	2.1	$0.1r_0^2$	3.6	$0.18r_0^2$
Fig. 5d	penguin-2g-op	1.0	$0.05r_0^2$	0.1	$0.005r_0^2$
Fig. 5e	tree	0.25	5.2	0.4	8.6
Total (no cuts)		354	$14r_0^2 + 8.6$	101	$1.6r_0^2 + 12$
Total (with cuts)		96	$4.2r_0^2 + 3.2$	17.6	$.54r_0^2 + 3.3$
$\frac{\text{Anomalous}}{\text{total}}$ (with cuts)		$\sim 86\%$	$\sim 55\%^a$	$\sim 44\%$	$\sim 10\%^a$

a) assuming  $r_0^2 = 1$ .

Figure 1



**Figure 2**

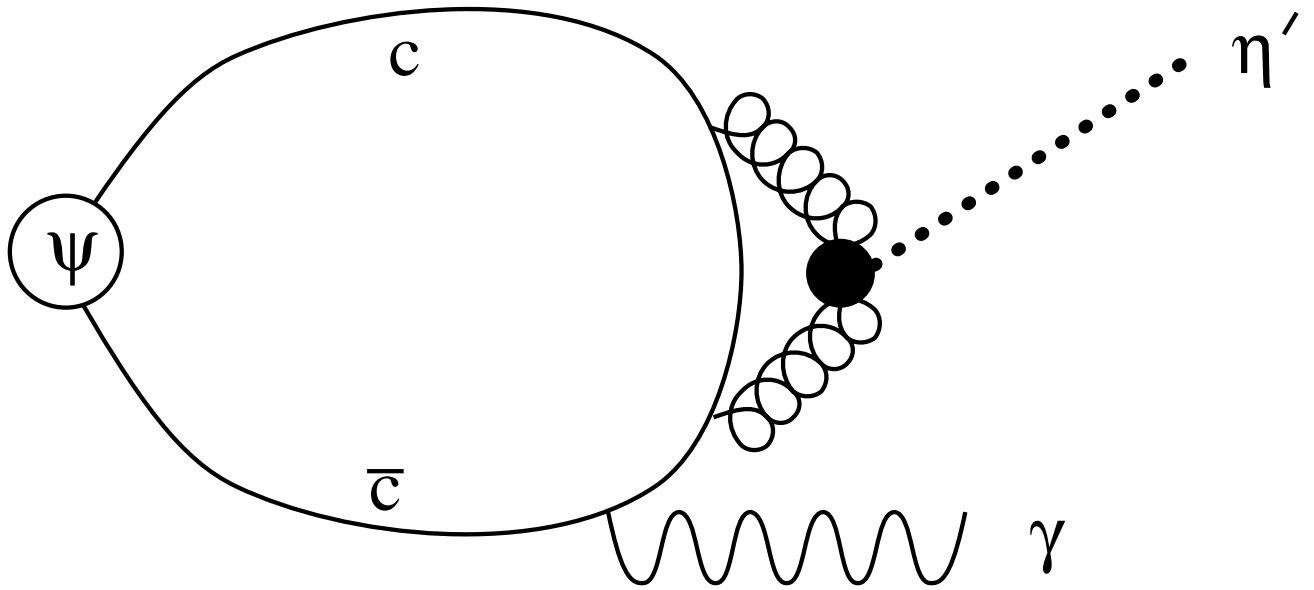




FIGURE 3

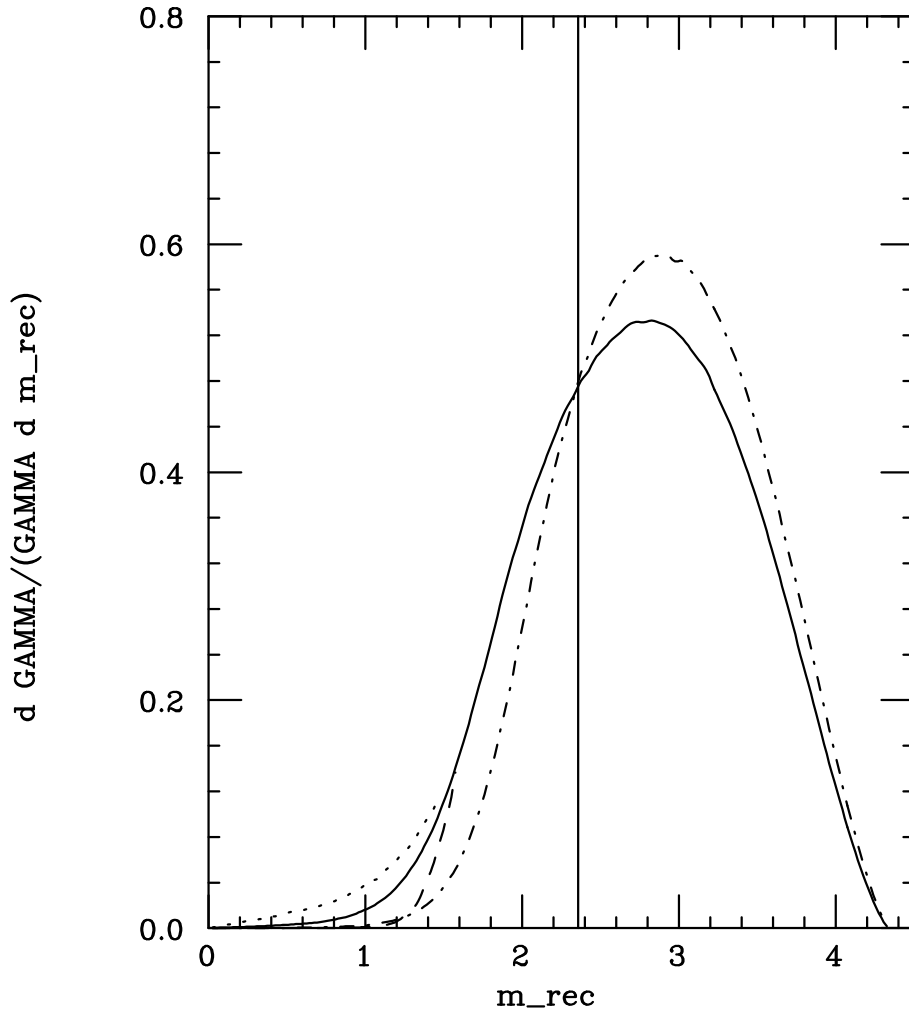
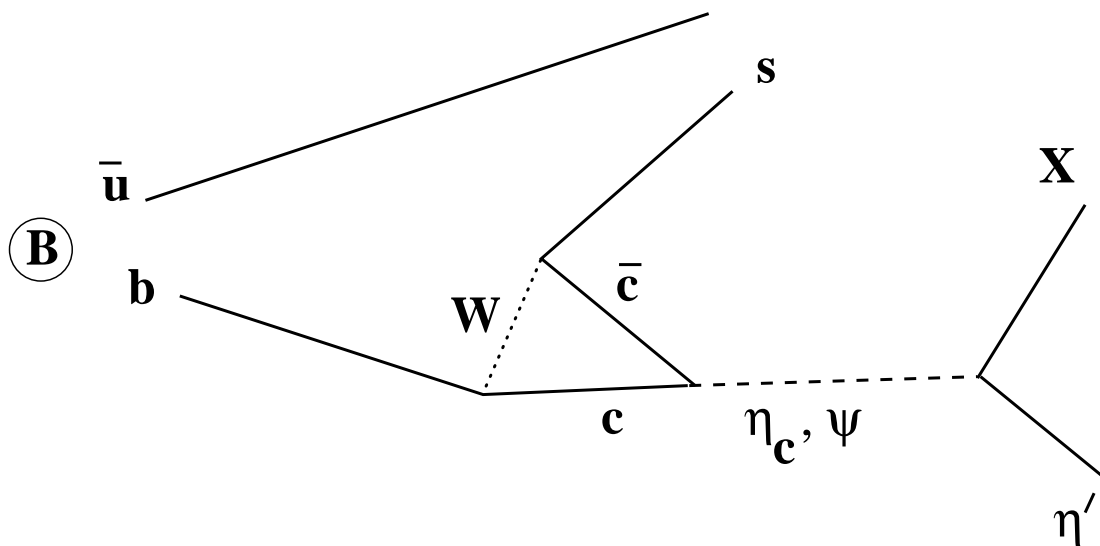
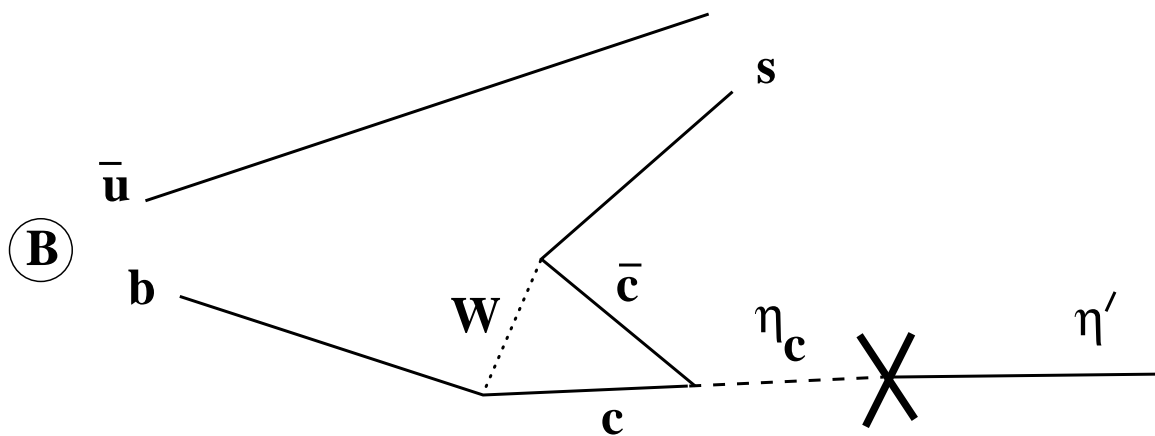


Figure 4



(4a)



(4b)

Figure 5

